Supporting Information for

Dynamically Wavelength-Tunable Random Lasers Based on Metal-organic Framework Particles

Baoyuan Xu,[a] Zhenhua Gao,*[a] Yanhui Wei,[b] Yang Liu,[a] Xun Sun,[a] Weiguang Zhang,[a] Xue Wang,[a] Zifei Wang,[a] Xiangeng Meng*[a]

a. School of Materials Science & Engineering, Qilu University of Technology (Shandong Academy of Sciences), 3501 Daxue Road, Changqing District, Jinan 250353, Shandong Province, China

b. College of Chemistry and Material Science, Shandong Agricultural University, Taian, 271018, Shandong, China

E-mail: gaozhenhua@qlu.edu.cn; mengxiangeng@gmail.com

Table of Contents

Materials and experimental Section

Materials: Trans-4-[4-(dimethylamino)styryl]-1-methylpyridinium iodide (DASPI), 4-[4-[4-(dimethylamino)phenyl]-1,3-butadienyl]-1-ethyl-pyridinium perchlorate (LDS722) and 2-[4-[4-(dimethylamino)phenyl]-1,3-butadienyl]-3-ethyl-naphtho[2,1-d]thiazolium perchlorate (LDS750) were purchased from Sigma-Aldrich and used without further purification. All the chemicals were used without further treatment.

Preparation: Three kinds of dissolved stock solutions, adenine (2.5 ml, 0.13 mmol) in DMF, Zinc acetate dehydrate (5 ml, 0.25 mmol) in DMF, Biphenyldicarboxylic acid (2.5 ml, 0.25 mmol) in DMF, were prepared by ultrasonication. Then, these three kinds of stock solutions were poured into a 20 ml vial with the late addition of 2.5 ml of DMF, 1ml of methanol and 0.25 ml of deionized water. The vial was capped and heated at 85 ℃ for 24 h and then cooled down to room temperature. The resultant product was rinsed with DMF three times and then dried in vacuum conditions, giving the Bio-MOF-100 crystalline powders. Crystals of Bio-MOF-100 were immersed in a solution of LDS 722 in DMF (0.45 mM) at 60 ℃ for 24 h to load LDS 722 into Bio-MOF-100. The resultant products were washed by DMF several times until there is no detectable PL signal in the supernatant. After being dried at 60 ℃ for 5 h, the crystals of LDS 722@Bio-MOF-100 were obtained. The preparation of DASPI@Bio-MOF-100 and LDS 750@Bio-MOF-100 undergoes the same steps mentioned above. The density of different dye molecules in the MOF systems were estimated according to the Beer-Lambert law. The dye molecule cations can be released from the MOF systems by exchanging cations with Li^+ and then comparing with the reference sample.[1] The calculated concentrations are 37.4, 27.1 and 18.8 $mmol \cdot L^{-1}$, respectively for the DASPI@MOF, LDS722@MOF and LDS750@MOF particles.

Characterizations: The morphology of the bio-MOF-100 particles was examined through scanning electron microscopy (Hitachi Regulus8220). The optical absorption and PL spectra were measured on a UV-visible spectrometer (SHIMADZU UV-3600 Plus) and a fluorescence spectrometer (EDINBURGH FLS1000), respectively. The transient PL decay spectra were measured on Edinburgh FLS1000 photoluminescence spectrometer

(Edinburgh Instruments, UK) equipped with a supercontinuum white light laser (Superk EXTREME, 2-80 MHz) as the light source, and the excitation wavelength was set as 532 nm (19.5 MHz). The decay curves detected at different wavelengths of 650, 700 and 800 nm within the PL band of LDS722@MOF, respectively. The dye concentration in sample of LDS722@MOF is 27.1 mmol·L^{-1}. A focused picosecond pulsed laser beam from an optical parametric generator (EKSPLA, PG-401) was employed to locally excite the dye@bio-MOF-100 composite particles and the spatially resolved spectra were recorded with a monochrometer (Princeton Instruments, SP-2500) connected with an CCD (Princeton Instruments, PIXIS 256). XRD measurements...

Calculations: The calculations were performed with Gaussian software on the basis of density functional theory (DFT) by using the ωB97XD functional and 6-311G (d,p) basis set.

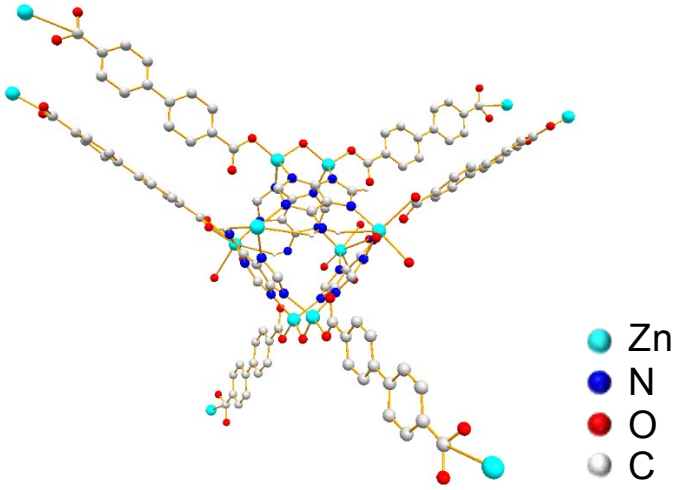

Figure S1. Molecular structure of bio-MOF-100. The structure of bio-MOF-100 consists of inorganic (Zn) and organic building blocks (adeninate (ad) and biphenyldicarboxylate (BPDC) linkers).[2] Eight Zn^{2+} cations are interconnected with four adeninates, two μ-oxo groups and six monodentate BPDCs, forming the molecular structure formulated as $Zn_8(ad)_4(BPDC)_6O_2{\cdot}4Me_2NH_2$. The framework has a net 4-charge per formular unit, resulting in the anionic microenvironment of bio-MOF-100.

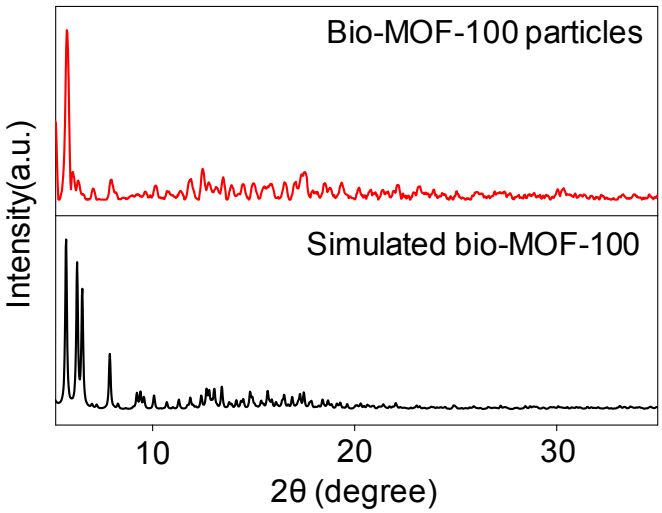

Fig. S2. X-ray powder diffraction patterns of bio-MOF-100: simulation (black curve) and experimental (red curve). The experimental results are well consistent with the simulated ones, suggesting that phase-pure bio-MOF-100 was obtained.

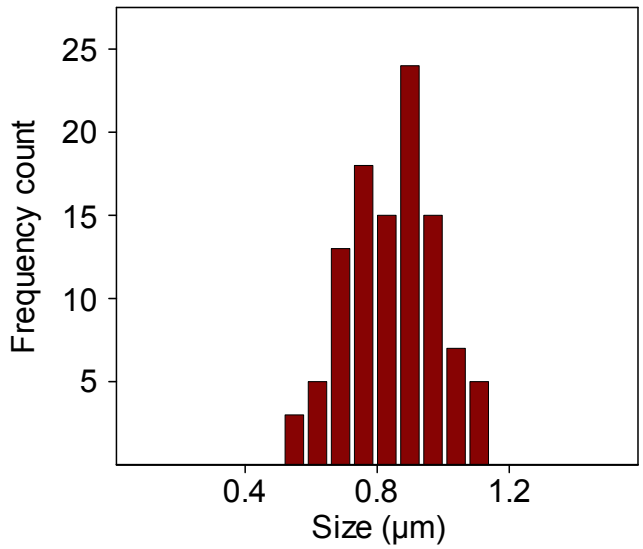

Fig. S3. Histogram for the size distribution of the MOF particles. The average size of the particles is determined to be about 0.8 ± 0.2 μm.

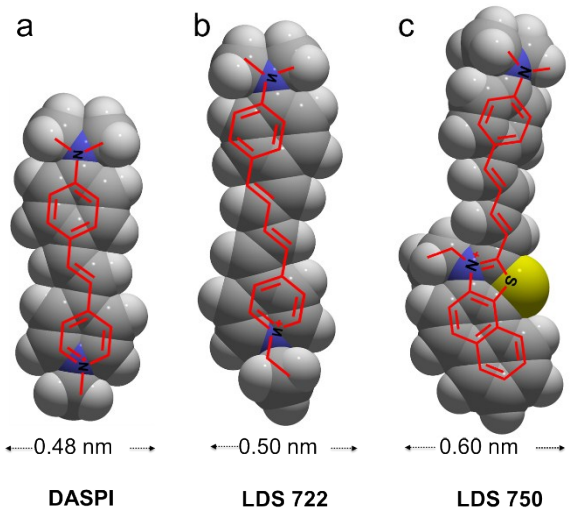

Figure S4. Geometries of DASPI, LAD 722 and LDS 750 molecules that are optimized on the ωB97XD/6-311G (d, p) level of theory. The lateral dimensions are determined to be 0.48, 0.50 and 0.60 nm for DASPI, LDS 722 and LDS 750 molecules, respectively.

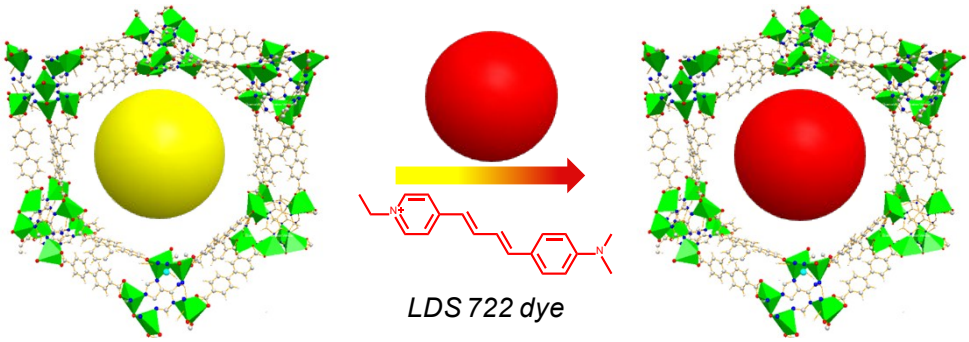

Figure S5. Schematics of an ion-exchange process that is used to introduce the cationic dye LDS 722 inside bio-MOF-100. The internal pores of bio-MOF-100 contain a large amount of $Me_2NH_2^+$ cations, thus allowing for facile incorporation of cationic dyes via strong ionic interaction.

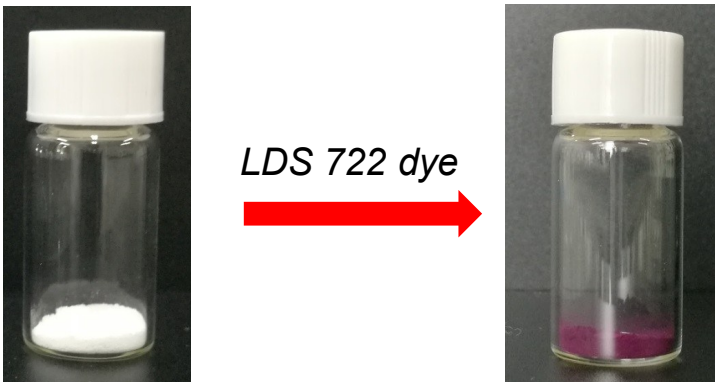

Figure S6. Digital photographs of bio-MOF-100 powders before and after introduction of LDS 722 dye. Owing to the strong ionic interaction, the MOFs exhibit an obvious color change from the original colorless to the final purple particles after the ion exchange, indicating that the LDS 722 laser dye were encapsulated into the bio-MOF-100 pores.

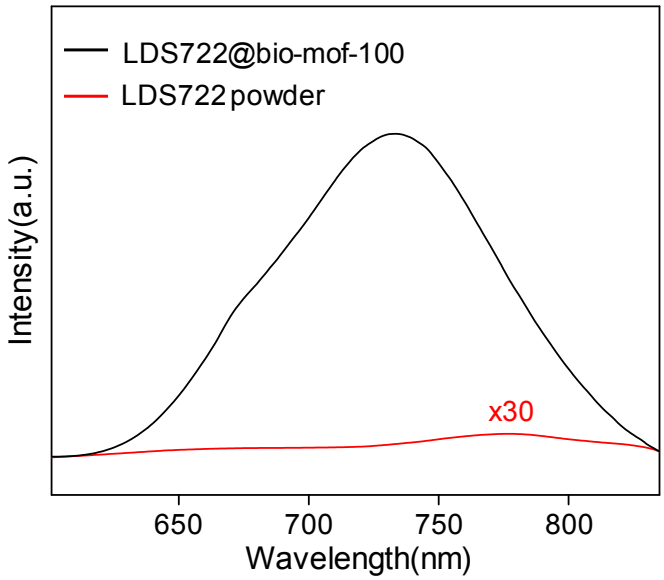

Figure S7. PL spectra of LDS722 and LDS722@bio-MOF-100 powders excited at 532 nm. The much stronger PL signal from LDS722 in bio-MOF-100 than bare LDS722 powders indicates the occurrence of an efficient monomer emission in the confined system. The restricted ICT dyes display strong red emission compared with that of LDS722 powder, indicating that the ICT dye molecules confined in the pores of MOFs have restricted intramolecular torsional motion and restrained π-π interactions,[3] providing a good candidate for high-performance random lasing.

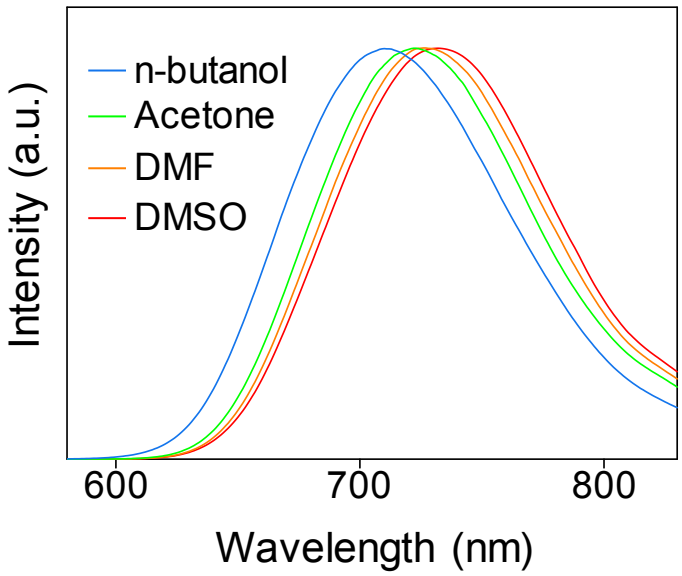

Figure S8. Normalized PL spectra of LDS 722 molecules in different solvents with increasing polarity (DMSO>DMF>Acetone>n-butanol). When the solvent polarity increased gradually from low-polarity n-butanol to high-polarity DMSO, the LDS 722 solution exhibits a large red-shift of 25 nm. This large solvatochromic shift, which is commonly consistent with the large dipole moment of the ICT state, indicates that the LDS 722 molecules possess a strong ICT state characteristic.[4]

Table S1. PL decay of LDS 722@bio-MOF100 particles at different wavelength.

	t_1 (ns)	w_1	t_2 (ns)	w_2	χ^2
650 nm	0.65	0.67	2.15	0.33	0.99
700 nm	0.72	0.58	2.21	0.42	0.99
800 nm	0.76	0.46	2.23	0.54	0.98

The PL decay curve of LDS 722@bio-MOF100 particles was best fitted with two exponential components, which indicates that the luminescence is originated from two excited states, namely LE state and TICT state.

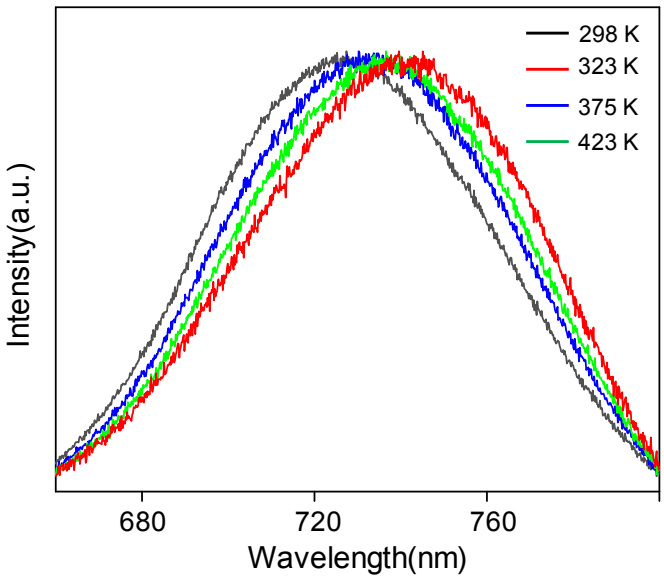

Figure S9. Temperature-dependent PL spectra of LDS 722@bio-MOF100 particles. The temperature-dependent PL spectra prove the feasibility of tuning the gain region in the MOF pellets, which can be utilized to build wavelength tunable random lasers.

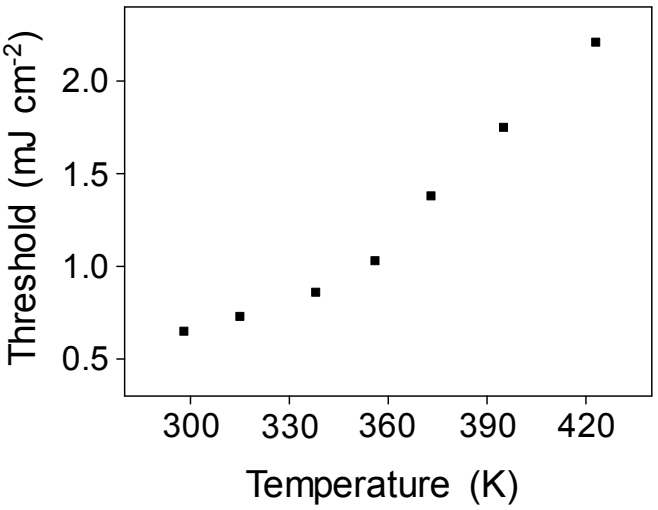

Figure S10. Threshold of the LDS 722@bio-MOF100 random lasers evaluated at different temperatures. The high temperature causes the additional nonradiative losses of LDS 722 dyes. Accordingly, the lasing threshold increases monotonically with temperature.

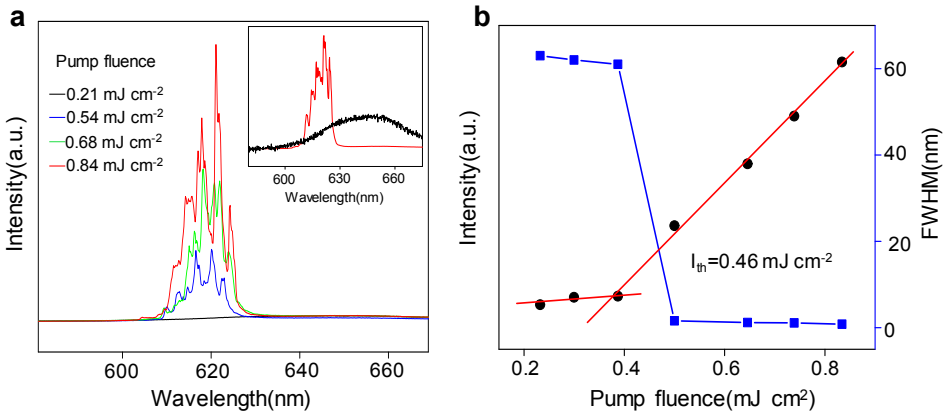

Figure S11. (a) Evolution of the emission spectral profile with the pump fluence for DASPI@bio-MOF-100 random lasers. Inset: Emission spectra recorded below (black) and above (red) the pump threshold. (b) Dependence of the emission intensity (red) and the spectral linewidth (blue) on the pump fluence.

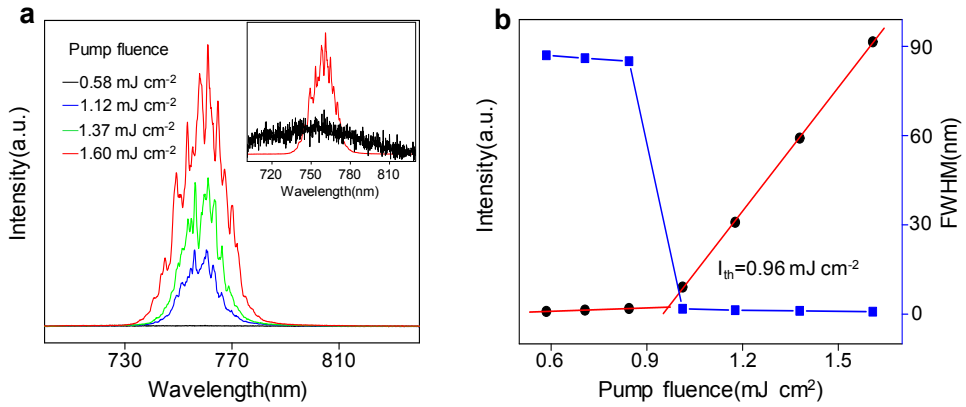

Figure S12. (a) Evolution of the emission spectral profile with the pump fluence for LDS750@bio-MOF-100 random lasers. Inset: Emission spectra recorded below (black) and above (red) the pump threshold. (b) Dependence of the emission intensity (red) and the spectral linewidth (blue) on the pump fluence.

References:

1. Y. Liu, H. Dong, K. Wang, Z. Gao, C. Zhang, X. Liu, Y. S. Zhao, F. Hu, *ACS Appl. Mater. Interfaces* 2018, **10**, 35455-35461.
2. J. An, O. K. Farha, J. T. Hupp, E. Pohl, J. I. Yeh, N. L. Rosi, *Nat. Commun.* 2012, **3**, 604.
3. Y. Wei, H. Dong, C. Wei, W. Zhang, Y. Yan, Y. S. Zhao, *Adv. Mater.* 2016, **28**, 7424-7429.
4. W. Li, D. Liu, F. Shen, D. Ma, Z. Wang, T. Feng, Y. Xu, B. Yang, Y. Ma, *Adv. Funct. Mater.* 2012, **22**, 2797-2803.